Ejection of Quasi-Free-Electron Pairs from the Helium-Atom Ground State by Single-Photon Absorption

M. S. Schöffler,[1,*] C. Stuck,[1,2] M. Waitz,[2] F. Trinter,[2] T. Jahnke,[2] U. Lenz,[2] M. Jones,[3] A. Belkacem,[1] A. L. Landers,[3] M. S. Pindzola,[3] C. L. Cocke,[4] J. Colgan,[5] A. Kheifets,[6] I. Bray,[7] H. Schmidt-Böcking,[2] R. Dörner,[2] and Th. Weber[1]

[1]*Lawrence Berkeley National Laboratory, Berkeley, California 94720, USA*
[2]*Institut für Kernphysik, University Frankfurt, Max-von-Laue-Strasse 1, 60438 Frankfurt, Germany*
[3]*Department of Physics, Auburn University, Auburn, Alabama 36849, USA*
[4]*Department of Physics, Kansas State University, Manhattan, Kansas 66506, USA*
[5]*Theoretical Division, Los Alamos National Laboratory, Los Alamos, New Mexico 87545, USA*
[6]*Research School of Physical Sciences and Engineering, Australian National University, Canberra, Australian Capital Territory 0200, Australia*
[7]*ARC Centre for Antimatter-Matter Studies, Curtin University, Perth, Western Australia 6845, Australia*

(Received 27 July 2012; published 2 July 2013)

We investigate the single-photon double ionization of helium at photon energies of 440 and 800 eV. We observe doubly charged ions with close to zero momentum corresponding to electrons emitted back to back with equal energy. These slow ions are the unique fingerprint of an elusive quasifree photon double ionization mechanism predicted by Amusia *et al.* nearly four decades ago [J. Phys. B **8**, 1248 (1975)]. It results from the nondipole part of the electromagnetic interaction. Our experimental data are supported by calculations performed using the convergent close-coupling and time-dependent close-coupling methods.

DOI: 10.1103/PhysRevLett.111.013003 PACS numbers: 32.80.Fb

The nonrelativistic Hamiltonian of electromagnetic interaction is a one-body operator and thus it couples one photon to just one electron. Simultaneous emission of two electrons following the absorption of a single photon is only possible due to electron-electron correlation. Single-photon double ionization (PDI) of helium became the prototype process to investigate such correlations. The two specific correlation mechanisms, the shakeoff (SO) and electron knockout processes (the latter is also known as two-step-1 or TS1 [1]), are well established today to facilitate the ejection of two electrons by a single photon. In both cases, the photon couples primarily to the dipole formed by one electron and the nucleus. The two electrons interact with each other, either before (SO) or after (TS1) the photoabsorption takes place. The energy sharing between the two emitted electrons is flat for low photon energies and exhibits a U shape [2,3], which becomes deeper and deeper with increasing photon energies [4–6]. The TS1 probability decreases with the increasing photon energy while the SO probability increases and finally saturates at the (nonrelativistic) shakeoff limit [7–11]. A common fingerprint of both mechanisms is a large momentum of the doubly charged ion and an almost dipolar angular distribution of the ion momentum with respect to the linear photon polarization axis. These two characteristic features are signatures of the initial coupling of the photon to the dipole formed by the primary electron and the nucleus [12–16].

Nearly four decades ago, Amusia *et al.* [2] predicted a third, so-called quasifree mechanism (QFM) of PDI. Its characteristic fingerprint is the ejection of two electrons back to back with similar energy while the nucleus is only a spectator remaining almost at rest [17–19]. They argued that this mechanism ejects electrons mainly from the part of the initial state wave function at the electron-electron cusp, i.e., where both electrons are spatially close together [17,20,21]. It is a contribution to the quadrupole part of PDI since emitting electrons back to back with equal energies is forbidden by the kinematic selection rule in a dipole transition [22]. This region of momentum space is, however, allowed in a quadrupole transition.

The QFM transition amplitude is extremely small, which is why it could not be verified experimentally so far. For instance, for a photon energy of 800 eV and the hydrogen Bohr radius, the nondipole transition amounts to 1% of the total PDI cross section only. From this quadrupole part, the QFM is only a small part; it can be estimated to 0.1% of the total PDI cross section [23,24].

The PDI of He in the low photon energy regime, where quadrupole transitions are negligible, has been investigated experimentally and theoretically in great detail in the past [25–27]. Experimental fully differential cross sections are available up to 530 eV [12,14,28–30]. However, very little is known about PDI at higher photon energies. The coupling of higher orders of angular momentum of the incoming light, such as the electric quadrupole term, to the two electrons in the atom has only been addressed theoretically [19,31–35]. So far, no experiments have studied nondipole effects in the PDI due to extremely small cross sections. As the QFM has an even smaller cross section and requires, in addition, the coincident detection of two electrons emitted back to back with equal energy, it escaped experimental observation until now.

In the present Letter, we report on the observation of low momentum doubly charged ions for the PDI of helium at 800 eV and thus present direct support for the QFM mechanism. This is also consistent with the accompanying *ab initio* nonperturbative calculations, performed using the convergent close-coupling (CCC) and the time-dependent close-coupling (TDCC) methods, which reproduce our experimental findings.

The experiments were carried out with linear polarized light at 800 eV during the two-bunch mode at beam line 11.0.2.1 of the Advanced Light Source of the Lawrence Berkeley National Laboratory. The technical realization of this project is very challenging. The cross section for quadrupole transitions amounts to $\simeq 2 \times 10^{-25}$ cm^2 only. At the same time, a coincidence measurement of the momentum vectors of at least one electron and the recoiling doubly charged ion is necessary to cleanly single out the scarce PDI events (total cross section $\simeq 2 \times 10^{-23}$ cm^2). The solution to this problem is the application of the cold target recoil ion momentum spectroscopy method which is able to detect the three-dimensional momenta of the outgoing particles within the 4π solid angle in coincidence [36–38]. It is sufficient to measure one electron and the recoiling ion simultaneously. Momentum conservation is used to calculate the momentum vector of the second electron and the energy conservation is exploited to eliminate background in the off-line analysis. In brief, the target is prepared in a supersonic gas jet (30 μm nozzle and 20 bar driving pressure) along the y direction and intersected with the photon beam (propagating along the x axis) in a weak electric field inside the momentum spectrometer. The field (16 V/cm) is just strong enough to separate the fragments by their charge and guide them toward two large position and time sensitive multichannel plate detectors with a delay line readout [39,40], an 80 mm diameter for the ions and 120 mm for the electrons. A magnetic field (23 G) in parallel is used to prevent high energy electrons from leaving the spectrometer by forcing these particles to gyrate toward the detector. With the knowledge of the dimensions of the spectrometer, the field strengths, the position of impact and time of flight of the particles, the three-dimensional momentum vector of each particle can be deduced. To increase the ion momentum resolution and to compensate for the finite interaction volume (see [41] for general information about the time and space focusing), we employed an electrostatic lens and a 120 cm long drift region for focusing. This resulted in an ion momentum resolution of $\simeq 0.15$ a.u. in the light polarization direction (z), which is also the time-of-flight direction, and $\simeq 0.25$ a.u. in the transverse direction. The axis layout is shown in Fig. 1(a). The photon beam had a small contamination of 100 eV photons. Because of an increase of the PDI cross section with decreasing photon energy, this small contamination leads to a non-negligible amount of low momentum doubly charged ions. Our coincidence

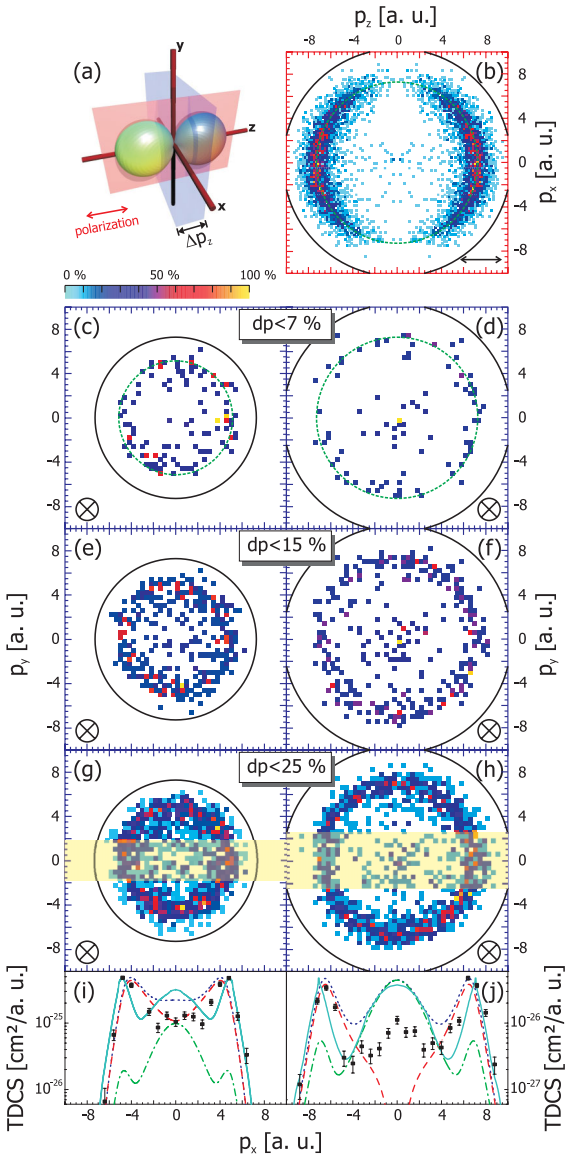

FIG. 1 (color online). (a) Sketch of the dipole structure, different planes and coordinates: light propagation x, light polarization z, gas jet direction y. (b) Slice ($|p_y| < 0.73$ a.u.) of the ion momentum distribution in the xz plane for $\hbar\nu = 800$ eV. (c)–(h) Ion momentum distribution perpendicular to the light polarization vector for $\hbar\nu = 440$ eV (left column) and $\hbar\nu = 800$ eV (right column), with different momentum intervals dp parallel to the polarization vector of the doubly charged ion at a given photon energy. (c),(d) $dp = 7\%$; (e),(f) $dp = 15\%$; (g),(h) $dp = 25\%$. The solid circular line represents the maximum possible momentum ($p_{\max}$). The dashed green line in (b)–(d) represents the case when one electron receives all momentum. Panels (i) and (j) show a projection of (g) and (h) to the horizontal p_x axis for a momentum interval of $|p_y/p_{\max}| \leq 25\%$ indicated by the yellow bars. The solid light blue line represents the CCC calculation for dipole + quadrupole, while the other lines show TDCC calculations for dipole (dashed and red), quadrupole (dash-dotted green), as well as the coherent sum of dipole and quadrupole (dotted blue). The experimental data have been normalized to Samson *et al.* [45]; the theory maximum has been normalized to the experiment maximum.

experiment, however, provides for each registered event the sum energy of both electrons. This has been used to identify the contamination of the ion signal by low energy photons and to unambiguously select events which resulted from the absorption of one 800 eV photon. This also discriminates against events from Compton scattering, which also would produce low momentum ions [13]. As our detection and reconstruction efficiency is not constant for all electron energies we performed a complete simulation of the spectrometer and a Monte Carlo simulation of the subsequent momentum analysis. These results were used to weigh the experimental data correctly. This procedure increased the intensity of zero momentum ions by about 50%.

In Fig. 1(b) we present the momentum distribution of the doubly charged helium ions after the PDI with linear polarized light of 800 eV. The solid circular line represents the maximum possible momentum an ion could receive in a double ionization [$p_{\max} = 2\sqrt{(E_\gamma - 79\ \text{eV})/2}$, where 79 eV represents the PDI threshold]. This is the case when both electrons have half the excess energy and are emitted in the same direction. Nevertheless, the vast majority of events are located close to the surface of a sphere in the momentum space with a radius of $p_{\text{single}} = \sqrt{E_\gamma - 79\ \text{eV}}$, which corresponds to the recoil momentum of one electron that takes away all the available energy. These ions show a close to dipolar angular distribution. This is the characteristic pattern observed in all previous experiments [12,15,16]. It is created by both the SO and TS1 process and dominated by the dipole transition by far. In the center of the sphere, close to the momentum zero, we expect the events from the QFM. To make those events more visible, we plot the two momentum components in the xy plane perpendicular to the polarization direction [Figs. 1(c)–1(e), 1(g), and 1(h)]. We restrict the momentum interval $dp = |\Delta p_z/p_{\max}|$ perpendicular to this plane (i.e., along the z direction) and show cuts corresponding to $dp = 7\%$, 15%, and 25% of the maximum momentum in Figs. 1(c)–1(h); respectively. Choosing this plane perpendicular to the linear polarization vector of the incoming light allows us to exploit the selection rules for the dipole transitions which forbid the emission of both electrons in the xy plane, irrespective of the energy sharing [22]. The outer ring of the pattern corresponds to transitions with maximum unequal electron energy sharing. In the center of this ring we find ions almost at rest, their relative contribution increases with the photon energy; compare the left column (440 eV) with the right column (800 eV). As outlined above, we have performed a kinematically complete experiment; i.e., we obtained the momentum vectors of all particles. This allows a full sampling of the experiment and a highly efficient suppression of all background. We therefore can be certain that the small amount of events at zero momentum is experimentally significant and definitely not background. A projection from Figs. 1(g) and 1(h) with an interval $dp = 25\%$ (indicated by the yellow bars) is shown in Figs. 1(i) and 1(j). Here a peak around zero momentum is clearly visible for 800 eV, but it is elusive for 440 eV. Why the calculations overestimate the experimental data for the QFM by a factor of 5 [Fig. 1(j)] is yet unknown.

The present experimental findings are supported by CCC calculations [42] and TDCC theory [43] shown in Fig. 2 for 440 (left) and 800 eV (right) photon energies and a cut in $p_z = \pm 15\%$. These calculations contain the dipole part [Figs. 2(a) and 2(b)] and quadrupole contributions

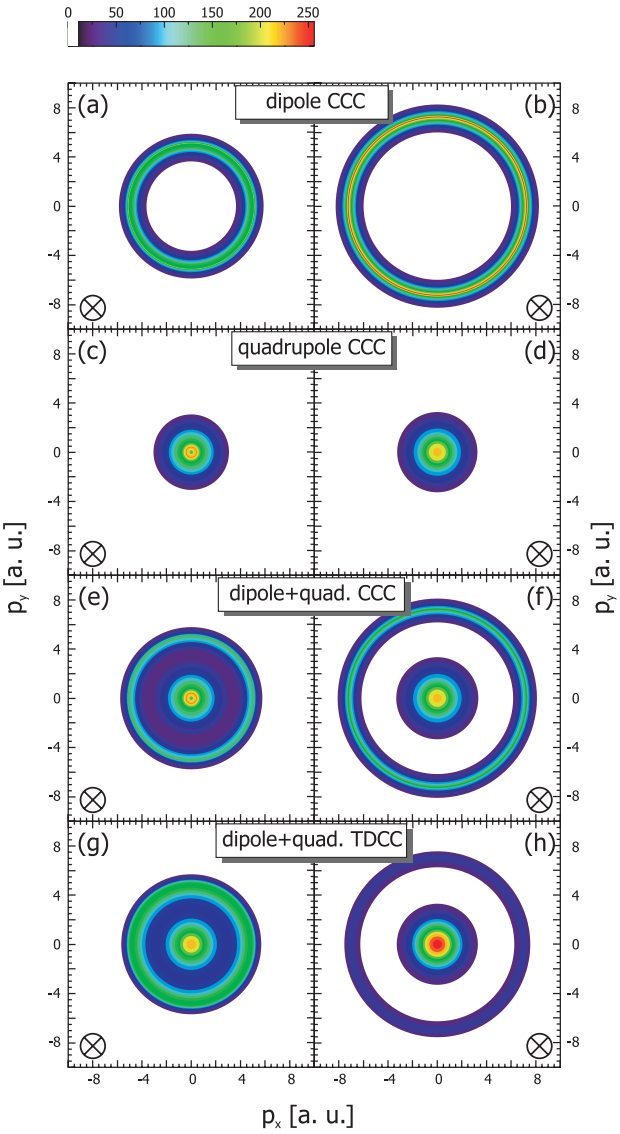

FIG. 2 (color online). Calculations for 440 (left column) and 800 eV (right column) photon energy with the same geometry as in the experiment [Figs. 1(e) and 1(f), for an interval of $dp = \pm 15\%$]. In panels (a) and (b) the CCC calculations include only the dipole interaction, while (c) and (d) solely display the quadrupole terms and (e) and (f) show the full theory. Panels (g) and (h) show a full TDCC calculation including dipole and quadrupole terms and in contrast to the CCC theory, their interference terms as well.

[Figs. 2(c) and 2(d)] as well as the coherent (TDCC) and incoherent (CCC) sum of the dipole and quadrupole matrix elements [Figs. 2(e) and 2(f)]. Both calculations show ions with zero momentum for the quadrupole, but not for the dipole terms. The individual dipole and quadrupole contributions from CCC and TDCC agree well. The higher momenta contain contributions from both the dipole and the quadrupole term. The TDCC is a direct solution of the time-dependent Schrödinger equation. It is not possible to connect this to the intuitive picture of ionization mechanisms. As the calculation is exact up to the quadrupole term, it does, however, include all the possible PDI mechanisms. The CCC calculations, in turn, can be analyzed in terms of Feynman diagrams [44]. Thus, the analysis of the mechanism in terms of the Feynman diagrams presented in the manuscript is in line with the one given in earlier publications [19,23].

In conclusion, we performed kinematically complete experiments on single-photon double ionization of helium at 440 and 800 eV with linearly polarized light. In contrast to all previous experimental work, we have observed, for the first time, ions with close to zero momentum, originating from a back-to-back emission of two electrons with equal energy sharing. This observation confirms the quasifree mechanism predicted nearly four decades ago by Amusia *et al.* [2]. Also our CCC and TDCC calculations confirm the existence of the QFM and show that these slow ions are produced by the quadrupole interaction with the photon field. Why both calculations overestimate the QFM is yet unknown. The newly observed double ionization mechanism probes the two electron wave function at the electron-electron cusp, a region previously inaccessible. These cusp electrons can be thought of as a bosonic electron pair, which is virtually free as they compensate completely each other's momentum, while the nucleus is at rest. When this pair is photoionized, a total energy of 720 eV, stored in the form of a Coulomb repulsion, is released.

We thank the staff of the Advanced Light Source, in particular H. Bluhm and T. Tyliszczak from beam line 11.0.2.1, for their outstanding support. M. S. Schöffler thanks the Alexander von Humboldt foundation for financial support. This work is supported by the Deutsche Forschungsgemeinschaft, DAAD, and the Office of Basic Energy Sciences, Division of Chemical Sciences, U.S. Department of Energy, and DOE-EPSCoR under Contracts No. DE-AC02-05CH11231 and No. DE-FG02-07ER46357. Resources of the Australian National Computational Infrastructure Facility were used in this work. The Los Alamos National Laboratory is operated by Los Alamos National Security, LLC for the NNSA of the U.S. DOE under Contract No. DE-AC5206NA25396. Computational work was carried out using Institutional Computing resources at Los Alamos National Laboratory. We thank Miron Y. Amusia for encouraging us for 16 years to perform the present experiment.

*schoeffler@atom.uni-frankfurt.de

[1] J. H. McGuire, *Electron Correlation Dynamics in Atomic Collisions*, Cambridge Monographs on Atomic, Molecular, and Chemical Physics (Cambridge University Press, Cambridge, 1997).
[2] M. Y. Amusia, E. G. Drukarev, V. G. Gorshkov, and M. P. Kazachkov, J. Phys. B **8**, 1248 (1975).
[3] D. Proulx and R. Shakeshaft, Phys. Rev. A **48**, R875 (1993).
[4] R. Wehlitz, F. Heiser, O. Hemmers, B. Langer, A. Menzel, and U. Becker, Phys. Rev. Lett. **67**, 3764 (1991).
[5] D. Proulx and R. Shakeshaft, Phys. Rev. A **48**, R875 (1993).
[6] T. Schneider, P. L. Chocian, and J.-M. Rost, Phys. Rev. Lett. **89**, 073002 (2002).
[7] P. K. Kabir and E. E. Salpiter, Phys. Rev. **108**, 1256 (1957).
[8] A. Dalgarno and A. L. Stewart, Proc. Phys. Soc. London **76**, 49 (1960).
[9] T. Åberg, Phys. Rev. **156**, 35 (1967).
[10] T. A. Carlson, Phys. Rev. **156**, 142 (1967).
[11] J. C. Levin, I. A. Sellin, B. M. Johnson, D. W. Lindle, R. D. Miller, N. Berrah, Y. Azuma, H. G. Berry, and D.-H. Lee, Phys. Rev. A **47**, R16 (1993).
[12] A. Knapp, A. Kheifets, I. Bray, T. Weber, A. L. Landers, S. Schössler, T. Jahnke, J. Nickles, S. Kammer, O. Jagutzki *et al.*, Phys. Rev. Lett. **89**, 033004 (2002).
[13] L. Spielberger, O. Jagutzki, R. Dörner, J. Ullrich, U. Meyer, V. Mergel, M. Unverzagt, M. Damrau, T. Vogt, I. Ali *et al.*, Phys. Rev. Lett. **74**, 4615 (1995).
[14] A. Knapp, A. Kheifets, I. Bray, T. Weber, A. L. Landers, S. Schössler, T. Jahnke, J. Nickles, S. Kammer, O. Jagutzki *et al.*, J. Phys. B **38**, 615 (2005).
[15] R. Dörner, J. M. Feagin, C. L. Cocke, H. Bräuning, O. Jagutzki, M. Jung, E. P. Kanter, H. Khemliche, S. Kravis, V. Mergel *et al.*, Phys. Rev. Lett. **77**, 1024 (1996).
[16] H. Bräuning, R. Dörner, C. L. Cocke, M. H. Prior, B. Krässig, A. Bräuning-Demian, K. Carnes, S. Dreuil, V. Mergel, P. Richard *et al.*, J. Phys. B **30**, L649 (1997).
[17] T. Suric, E. G. Drukarev, and R. H. Pratt, Phys. Rev. A **67**, 022709 (2003).
[18] M. Y. Amusia and E. G. Drukarev, J. Phys. B **36**, 2433 (2003).
[19] M. Y. Amusia, E. G. Drukarev, and E. Z. Liverts, JETP Lett. **96**, 70 (2012).
[20] M. Y. Amusia, E. G. Drukarev, and V. B. Mandelzweig, Phys. Scr. **72**, C22 (2005).
[21] E. G. Drukarev, Phys. Usp. **50**, 835 (2007).
[22] F. Maulbetsch and J. S. Briggs, J. Phys. B **28**, 551 (1995).
[23] E. G. Drukarev, Phys. Rev. A **51**, R2684 (1995).
[24] E. G. Drukarev (private communication).
[25] J. S. Briggs and V. Schmidt, J. Phys. B **33**, R1 (2000).
[26] L. Malegat, Phys. Scr. **T110**, 83 (2004).
[27] L. Avaldi and A. Huetz, J. Phys. B **38**, S861 (2005).
[28] A. Knapp, M. Walter, T. Weber, A. L. Landers, S. Schössler, T. Jahnke, M. Schöffler, J. Nickles, S. Kammer, O. Jagutzki *et al.*, J. Phys. B **35**, L521 (2002).
[29] A. Knapp, A. Kheifets, I. Bray, T. Weber, A. L. Landers, S. Schössler, T. Jahnke, J. Nickles, S. Kammer, O. Jagutzki *et al.*, J. Phys. B **38**, 635 (2005).

[30] A. Knapp, B. Krässig, A. Kheifets, I. Bray, T. Weber, A. L. Landers, S. Schössler, T. Jahnke, J. Nickles, S. Kammer *et al.*, J. Phys. B **38**, 645 (2005).
[31] A. I. Mikhailov, I. A. Mikhailov, A. N. Moskalev, A. V. Nefiodov, G. Plunien, and G. Soff, Phys. Lett. A **316**, 395 (2003).
[32] A. I. Mikhailov, I. A. Mikhailov, A. N. Moskalev, A. V. Nefiodov, G. Plunien, and G. Soff, Phys. Rev. A **69**, 032703 (2004).
[33] A. Y. Istomin, N. L. Manakov, A. V. Meremianin, and A. F. Starace, Phys. Rev. Lett. **92**, 063002 (2004).
[34] A. Y. Istomin, N. L. Manakov, A. V. Meremianin, and A. F. Starace, Phys. Rev. A **71**, 052702 (2005).
[35] A. G. Galstyan, O. Chuluunbaatar, Y. V. Popov, and B. Piraux, Phys. Rev. A **85**, 023418 (2012).
[36] J. Ullrich, R. Moshammer, R. Dörner, O. Jagutzki, V. Mergel, H. Schmidt-Böcking, and L. Spielberger, J. Phys. B **30**, 2917 (1997).
[37] R. Dörner, V. Mergel, O. Jagutzki, L. Spielberger, J. Ullrich, R. Moshammer, and H. Schmidt-Böcking, Phys. Rep. **330**, 95 (2000).
[38] J. Ullrich, R. Moshammer, A. Dorn, R. Dörner, L. P. H. Schmidt, and H. Schmidt-Böcking, Rep. Prog. Phys. **66**, 1463 (2003).
[39] O. Jagutzki, J. Lapington, L. Worth, U. Spillman, V. Mergel, and H. Schmidt-Böcking, Nucl. Instrum. Methods Phys. Res., Sect. A **477**, 256 (2002).
[40] O. Jagutzki, V. Mergel, K. Ullmann-Pfleger, L. Spielberger, U. Spillmann, R. Dörner, and H. Schmidt-Böcking, Nucl. Instrum. Methods Phys. Res., Sect. A **477**, 244 (2002).
[41] M. S. Schöffler, T. Jahnke, J. Titze, N. Petridis, K. Cole, L. P. H. Schmidt, A. Czasch, O. Jagutzki, J. B. Williams, C. L. Cocke *et al.*, New J. Phys. **13**, 095013 (2011).
[42] I. Bray, D. V. Fursa, A. S. Kadyrov, A. T. Stelbovics, A. S. Kheifets, and A. M. Mukhamedzhanov, Phys. Rep. **520**, 135 (2012).
[43] J. A. Ludlow, J. Colgan, T.-G. Lee, M. S. Pindzola, and F. Robicheaux, J. Phys. B **42**, 225204 (2009).
[44] A. Kheifets, J. Phys. B **34**, L247 (2001).
[45] J. A. R. Samson, W. C. Stolte, Z.-X. He, J. N. Cutler, Y. Lu, and R. J. Bartlett, Phys. Rev. A **57**, 1906 (1998).